REVEILLE 7 inhibits the expression of the circadian clock gene *EARLY FLOWERING 4* to fine-tune hypocotyl growth in response to warm temperatures

Ying-Ying Tian[1], Wei Li[1], Mei-Jing Wang[1], Jin-Yu Li[1], Seth Jon Davis[2,3], and Jian-Xiang Liu[1,*]

[1]State Key Laboratory of Plant Physiology and Biochemistry, College of Life Sciences, Zhejiang University, Hangzhou 310027, China.

[2]State Key Laboratory of Crop Stress Adaptation and Improvement, School of Life Sciences, Henan University, Kaifeng 475004, China.

[3]Department of Biology, University of York, Heslington, York, YO105DD, UK.

[*]Correspondence：jianxiangliu@zju.edu.cn

Article type:

Research article

Short title: RVE7 regulates thermomorphogenesis

Summary for the icon: Warm temperature–induced RVE7 fine-tunes thermoresponsive hypocotyl growth by inhibiting the expression of *ELF4* in *Arabidopsis*, indicating that ELF4 is important for thermomorphogenesis in plants.

Ying-Ying Tian, 0000-0002-1193-8622

Wei Li, 0000-0001-9692-6139

Mei-Jing Wang, 0000-0002-1233-5348

Jin-Yu Li, 0000-0002-6569-3659

Seth Jon Davis, 0000-0001-5928-9046

Jian-Xiang Liu, 0000-0003-0791-1301

Abstract

The circadian clock maintains the daily rhythms of plant growth and anticipates predictable ambient temperature cycles. The evening complex (EC), comprising EARLY FLOWERING 3 (ELF3), ELF4, and LUX ARRHYTHMO, plays an essential role in suppressing thermoresponsive hypocotyl growth by negatively regulating PHYTOCHROME INTERACTING FACTOR 4 (PIF4) activity and its downstream targets in *Arabidopsis thaliana*. However, how EC activity is attenuated by warm temperatures remains unclear. Here, we demonstrate that warm temperature–induced REVEILLE 7 (RVE7) fine-tunes thermoresponsive growth in Arabidopsis by repressing *ELF4* expression. *RVE7* transcript and RVE7 protein levels increased in response to warm temperatures. Under warm temperature conditions, an *rve7* loss-of-function mutant had shorter hypocotyls, while overexpressing *RVE7* promoted hypocotyl elongation. PIF4 accumulation and downstream transcriptional effects were reduced in the *rve7* mutant but enhanced in *RVE7* overexpression plants under warm conditions. RVE7 associates with the evening element in the *ELF4* promoter and directly represses its transcription. *ELF4* is epistatic to *RVE7*, and overexpressing *ELF4* suppressed the phenotype of the *RVE7* overexpression line under warm temperature conditions. Together, our results identify RVE7 as an important regulator of thermoresponsive growth that functions (in part) by controlling *ELF4* transcription, highlighting the importance of ELF4 for thermomorphogenesis in plants.

Keywords: *Arabidopsis thaliana*, ELF4, Hypocotyl growth, RVE7, Warm temperatures

Introduction

Plant growth and development are widely influenced by environmental conditions, including ambient temperatures (Vu et al., 2019). Plants sense elevated ambient temperatures and transduce the warm temperature signal to downstream transcription factors to regulate gene expression and trigger various physiological responses. These responses include rapid hypocotyl/petiole growth, increased leaf hyponasty, and accelerated flowering via a process known as thermomorphogenesis (Casal and Balasubramanian, 2019; Sun et al., 2020; Wang et al., 2021).

In Arabidopsis (*Arabidopsis thaliana*), warm temperatures are sensed by at least three thermosensors: phytochrome B (phyB), EARLY FLOWERING 3 (ELF3), and PHYTOCHROME INTERACTING FACTOR 7 (PIF7) (Lin et al., 2020). phyB and ELF3 are repressors of the transcription factor PIF4, which plays a key role in thermomorphogenesis (Jung et al., 2016; Legris et al., 2016). phyB, a well-known photoreceptor, rapidly reverts from its active form Pfr to its inactive form Pr under warm temperature conditions (Klose et al., 2020), which reduces its inhibition of PIF4 (Jung et al., 2016; Legris et al., 2016). ELF3 undergoes liquid–liquid phase separation (deactivation) and ubiquitin-mediated degradation under warm temperature conditions (Jung et al., 2020; Zhang et al., 2021b; Zhang et al., 2021c), both of which release the inhibitory effects of ELF3 on PIF4 (Nomoto et al., 2012; Box et al., 2015; Nieto et al., 2015; Jung et al., 2020; Silva et al., 2020). PIF7 was recently reported as a new type of thermosensor in Arabidopsis (Chung et al., 2020). Indeed, the secondary structure of *PIF7* RNA in the 5′ untranslated region (5′ UTR) undergoes a conformational change under warm temperature conditions, which leads to enhanced translation of PIF7 (Chung et al., 2020). Both PIF7 and PIF4 are basic helix-loop-helix (bHLH) transcription factors that recognize G-box (CACGTG)-containing *cis*-elements and regulate the transcription of

downstream genes involved in auxin biosynthesis and signaling to promote thermoresponsive hypocotyl growth (Gray et al., 1998; Franklin et al., 2011; Sun et al., 2012).

ELF3, together with ELF4 and LUX ARRHYTHMO (LUX), assemble into the evening complex (EC) to regulate the circadian clock (Thines and Harmon, 2010; Huang and Nusinow, 2016). LUX is a MYB domain transcription factor that binds to DNA with high affinity. However, the LUX-ELF3 complex has relatively poor DNA binding activity, but adding ELF4 to this complex restores its DNA-binding activity in *in vitro* DNA binding assays (Silva et al., 2020). Similarly, the complete EC strongly binds to DNA at 4°C and weakly binds to DNA at 27°C *in vitro*. Adding an excess of ELF4 restores strong DNA binding for the EC, even at 27°C (Silva et al., 2020), suggesting that ELF4 is a key modulator of thermosensitive EC activity. However, how ELF4 functions in thermomorphogenesis in plants has not yet been reported.

The circadian clock consists of a series of repressors and activators that form interconnected feedback loops (Zhang et al., 2021a). Besides the EC repressor, other transcription factors from the MYB family are also key components of the circadian clock. In particular, CIRCADIAN CLOCK ASSOCIATED 1 (CCA1) and LATE ELONGATED HYPOCOTYL (LHY) are transcriptional repressors belonging to a small MYB subfamily, which also includes eight REVEILLE (RVE) transcription factors (Rawat et al., 2009). Among the RVEs, RVE4/6/8 were shown to be activators of gene expression that act antagonistically with CCA1/LHY within the plant oscillator network to provide rhythmic robustness across environmental conditions (Xie et al., 2014; Shalit-Kaneh et al., 2018). RVE7, also known as EARLY-PHYTOCHROME-RESPONSIVE 1 (EPR1), was previously reported to primarily function as a circadian output rather than a circadian regulator at ambient temperature conditions (23°C) (Kuno et al., 2003).

In the current study, we uncovered the essential role of warm-induced RVE7 in thermomorphogenesis. We demonstrate that RVE7 represses the expression of the circadian clock gene *ELF4* and fine-tunes hypocotyl growth under warm temperature conditions. Thus, RVE7 is not only an output factor, as previously described, but it is also an important modulator of the circadian clock under specific thermal conditions.

Results

RVE7 promotes thermoresponsive hypocotyl elongation in Arabidopsis

Similar to *CCA1*/*LHY*, the expression of *RVE1*/*2*/*3*/*4*/*8*, but not *RVE5*/*6*, is regulated by the circadian clock in seedlings, with an expression peak occurring near subjective dawn at ambient temperature (Rawat et al., 2011). We examined the expression levels of these genes under ambient (22°C) and warm (29°C) temperature conditions. At ZT24 (zeitgeber time: 24 h, or dawn), the expression of *CCA1*/*LHY*/*RVE1*/*3*/*4*/*8* decreased while that of *RVE2* increased at 29°C (Figure S1). The expression of *RVE5*/*6* decreased slightly at ZT16 and ZT24 but increased slightly at ZT32 at 29°C compared to at 22°C (Figure S1). By contrast, the expression of *RVE7* increased at ZT16, ZT24, and ZT32 under warm temperature conditions (Figure 1A). These differences in *RVE7* transcript levels under warm conditions prompted us to focus on this gene.

Since heat stress elements (HSEs; 5′-AGAAnnTTCT-3′) are present in the upstream sequences of *RVE7*, we measured the expression of *RVE7* at ZT24 in a quadruple knockout (qk) mutant of Arabidopsis *HEAT SHOCK FACTOR A1* (*HSFA1*) genes (*HSFA1A*, *HSFA1B*, *HSFA1C*, and *HSFA1D*). *RVE7* expression did not increase in *hsfa1qk* seedlings at 29°C as it did in the wild type (WT; Figure 1B). Therefore, the induction of *RVE7* expression by warm temperatures is dependent on these HSFA1s. We then examined RVE7 protein accumulation under warm temperature conditions in seedlings overexpressing

RVE7-MYC driven by the constitutive cauliflower mosaic virus (CaMV) 35S promoter (Figure S2A) via immunoblot analysis. RVE7-MYC protein levels in these seedlings were higher at 29°C than at 22°C (Figure 1C), suggesting that RVE7-MYC might be degraded at 22°C. Indeed, RVE7-MYC was stabilized at 22°C when MG132, a potent 26S proteasome inhibitor, was added to the assays (Figure S3). We concluded that both *RVE7* transcript levels and RVE7 protein stability are regulated by warm temperatures.

To investigate the role of RVE7 in warm temperature–mediated growth, we generated two independent alleles (*rve7-11* and *rve7-12*) via clustered regularly interspaced short palindromic repeats (CRISPR)/CRISPR-associated nuclease 9 (Cas9)-mediated gene editing (Figure S4). The hypocotyl lengths of both the *rve7-11* and *rve7-12* mutants were similar to that of WT seedlings at 22°C. However, the hypocotyls of *rve7-11* and *rve7-12* seedlings were significantly shorter than those in WT at 29°C ($P < 0.05$, Figure 1D and F). We also generated *RVE7* overexpression lines (Figure S2A) and measured their hypocotyls. Consistent with the notion that RVE7 promotes hypocotyl growth at warm temperatures, the *RVE7* overexpression seedlings (*RVE7*ox-1 and *RVE7ox*-2 lines) were about 1.5-fold taller than WT seedlings at 29°C, but not at 22°C (Figure 1E and G). Taken together, these results demonstrate that RVE7 is a positive regulator of thermomorphogenesis that is important for hypocotyl growth under warm conditions.

RVE7 functions upstream of PIF4 during thermomorphogenesis

The bHLH transcription factor PIF4 is a central regulator of seedling and plant morphogenesis (Koini et al., 2009; Quint et al., 2016). To analyze the genetic relationship between *RVE7* and *PIF4*, we generated the *rve7-11 pif4-101* double mutant and performed an epistatic analysis. Similar to the *pif4-101* single mutant, the hypocotyls of *rve7-11 pif4-101* seedlings did not elongate at 29°C relative to seedlings grown at 22ºC (Figure 2A and C). Thus, *PIF4* is

epistatic to *RVE7* during thermomorphogenesis. To examine whether the effect of *RVE7* in promoting thermomorphogenesis depends on *PIF4*, we overexpressed *RVE7* in both the WT (*RVE7ox*) and *PIF4* mutant backgrounds (*pif4-101 RVE7ox*) (Figure S2B) and measured hypocotyl length. Unlike the *RVE7* overexpression seedlings in the WT background, the hypocotyl length of *pif4-101 RVE7ox* seedlings was similar to that in WT at 29°C (Figure 2B and D). Thus, the function of RVE7 in controlling thermoresponsive hypocotyl growth is largely dependent on PIF4.

To investigate how RVE7 affects PIF4 activity under warm temperature conditions, we performed reverse transcription quantitative PCR (RT-qPCR) and immunoblot analysis of WT, *rve7-11*, and *RVE7ox-1* seedlings. Compared to the WT, the expression of *PIF4* was higher in *RVE7ox-1* seedlings but lower in *rve7-11* seedlings at 29°C, whereas such differences were modest at 22°C (Figure 3A-B). In agreement with these results, the accumulation of endogenous PIF4 protein decreased in *rve7-11* seedlings and increased in *RVE7ox-1* seedlings only at 29°C (Figure 2E-F).

We also measured the expression levels of genes that function downstream of PIF4 (Wang et al., 2018). In agreement with the accumulation of PIF4 at 29°C, the transcript levels of At1g73120 (encoding an F-box protein), *XYLOGLUCAN ENDOTRANSGLYCOSYLASE 7* (*XTR7*, At4g14130), (*IAA19*, At3g15540), and *YUCCA 8* (*YUC8*, At4g28720) were higher in *RVE7ox-1* seedlings at 29°C compared to WT seedlings (Figure 3C, E, G, I). By contrast, At1g73120 and *XTR7* transcript levels were lower in *rve7-11* seedlings at this temperature (Figure 3D, F). We observed little effect on *IAA19* or *YUC8* transcript levels in *rve7-11* seedlings (Figure 3H, J), likely due to the functional redundancy of PIF4 with other regulators such as PIF5/7 (Koini et al., 2009; Fiorucci et al., 2020). The differences in the expression levels of the abovementioned genes among WT, *rve7-11*, and *RVE7ox-1* seedlings were

modest at 22°C (Figure 3C-J). Taken together, these results support the notion that RVE7 functions upstream of PIF4 in thermomorphogenesis to control PIF4 accumulation and the expression of its downstream target genes under warm temperature conditions.

RVE7 regulates the expression of the circadian clock gene *ELF4* under warm conditions

ELF3 inhibits PIF4 by both suppressing its accumulation via the EC (Nomoto et al., 2012) and preventing PIF4 from activating its transcriptional targets independently of the complete EC (Nieto et al., 2015). Therefore, we measured the expression levels of clock genes, including the three EC genes, in WT, *rve7-11*, and *RVE7ox-1* seedlings at both 22°C and 29°C. At 29°C, the expression of *ELF4* decreased at ZT16, ZT20, and ZT24 in *RVE7ox-1* seedlings but increased at ZT16 and ZT24 in *rve7-11* seedlings, relative to the WT (Figure 4A-B). However, the expression levels of *ELF4* in WT and *rve7-11* seedlings were similar at 22°C, while the expression levels of *ELF4* were lower in *RVE7ox-1* compared to WT seedlings at 22°C (Figure 4A-B). By contrast, the expression levels of both *ELF3* and *LUX* were similar between WT, *rve7-11*, and *RVE7ox-1* seedlings at both 22°C and 29°C (Figure 4C-F). The expression levels of *ELF4* were lower in *RVE7ox-1* seedlings at ZT16 and ZT20 at 22°C, likely because *RVE7* was constitutively overexpressed in these lines. Finally, the expression of *ELF4* was anti-phase to the expression of *RVE7* and *PIF4* in WT seedlings, both at 22°C and 29°C (Figure S5). Together, these results indicate that RVE7 regulates *ELF4* expression under warm temperature conditions.

RVE7 directly binds to the evening element (EE) in the *ELF4* promoter and inhibits transcription

To explore how RVE7 regulates gene expression, we performed an effector-reporter assay with the *ELF4* promoter region (Figure 5A). RVE7 exhibited a

similar repressor activity as CCA1 in this assay (Figure 5B). We then performed electrophoretic mobility shift assays (EMSAs) using recombinant purified maltose binding protein (MBP)-RVE7 and the biotin-labeled clock gene-associated *cis*-element Evening Element (EE) derived from the *ELF4* promoter. When MBP-RVE7 was incubated with biotin-labeled EE (5′-AAATATCT-3′), we observed a shift in mobility for the labeled probe (Figure 5C). Adding non-labeled cold probes competed with this binding, while adding the mutated form (5′-AAATCGAG-3′) as a cold probe did not (Figure 5C), indicating that the binding of MBP-RVE7 to the EE is sequence specific. These results demonstrate that RVE7 specifically binds to the *ELF4* promoter via the EE.

To examine the *in vivo* binding of RVE7 to the *ELF4* promoter, we performed chromatin immunoprecipitation qPCR (ChIP-qPCR) using *RVE7-MYC* overexpression lines grown at both 22°C and 29°C. After the RVE7-MYC fusion protein was precipitated, we successfully amplified the *ELF4* genomic sequence (–364 bp to –170 bp relative to the TSS [transcription start site]) by PCR (Figure 5D). Thus, RVE7 binds to the *ELF4* promoter *in planta*. Furthermore, warm temperatures enhanced the occupancy of RVE7 at *ELF4* (Figure 5D). Since CCA1 and LHY were previously shown to associate with the *PIF4* promoter (Sun et al., 2019), we also examined the possible *in vivo* binding of RVE7-MYC to the *PIF4* promoter. We detected a slight enrichment of RVE7-MYC at the *PIF4* promoter region (–577 to –415 bp relative to the TSS) at 29°C (Figure S6). Therefore, RVE7 directly inhibits the expression of *ELF4* by binding to the EE *cis*-element in its promoter at warm temperatures.

Overexpressing *ELF4* alleviates the inhibitory effect of RVE7 on hypocotyl growth under warm temperature conditions

To explore the genetic relationship between *RVE7* and *ELF4*, we generated the *rve7-11 elf4-209* double mutant and performed a phenotypic analysis under warm temperature conditions. *elf4-209* seedlings (Kolmos et al., 2009) had long

hypocotyls at both 22°C and 29°C, while *rve7-11* seedlings had short hypocotyls at 29°C (Figure 6A-B). By contrast, the hypocotyl length of *rve7-11 elf4-209* seedlings was similar to that of *elf4-209* seedlings at both 22°C and 29°C (Figure 6A-B). Thus, *ELF4* is epistatic to *RVE7*. We also generated lines overexpressing both *RVE7* and *ELF4* (Figure S2C) and determined that overexpressing *ELF4* partially suppresses the long hypocotyl phenotype caused by *RVE7* overexpression at warm temperatures (Figure 6C-D). Seedlings overexpressing *RVE7* had long hypocotyls at 29°C (Figure 1E, G). We crossed the *RVE7ox-3* overexpression line with the *elf4-209* mutant and performed a phenotypic analysis. The hypocotyl length of *elf4-209 RVE7ox-3* seedlings was similar to that of *elf4-209* seedlings at both 22°C and 29°C (Figure 6E-F). Finally, we measured PIF4 abundance in *RVE7* and *ELF4* double overexpression lines under warm temperature conditions. Overexpressing *ELF4* prevented PIF4 accumulation, while overexpressing *RVE7* had the opposite effect. However, overexpressing *ELF4* suppressed PIF4 accumulation in *RVE7* overexpression lines at 29°C (Figure 6G-H). These results confirm the notion that RVE7 regulates hypocotyl growth by inhibiting the expression of clock genes such as *ELF4* under warm temperature conditions.

RVE7 functions redundantly with CCA1/LHY in controlling hypocotyl growth under warm temperature conditions

CCA1 and *LHY* play partially redundant functions in maintaining circadian rhythms and controlling temperature compensation in Arabidopsis (Mizoguchi et al., 2002; Salome et al., 2010). CCA1 and LHY play negative roles in light-induced *ELF4* expression (Kikis et al., 2005), and CCA1 represses *ELF3* expression by associating with its promoter. ELF3 acts downstream of CCA1 to mediate the repression of *PIF4* and *PIF5* to control hypocotyl elongation under ambient temperature conditions (Lu et al., 2012). Therefore, we

investigated the possible functional redundancy between RVE7 and CCA1/LHY. The hypocotyls of the *cca1 lhy* double mutant are shorter than those of WT seedlings when grown at 22°C under red-light conditions (Yamashino et al., 2008). However, under white light conditions at 20°C, the difference in hypocotyl length between WT and *cca1 lhy* plants is marginal (Sun et al., 2019). We crossed *rve7-11* to the *cca1-1 lhy-20* double mutant (Marshall et al., 2016) and generated the *rve7-11 cca1-1* and *rve7-11 lhy-20* double mutants, as well as the *rve7-11 cca1-1 lhy-20* triple mutant, and measured their hypocotyl lengths at both 22°C and 29°C. The hypocotyl lengths of the *cca1-1* and *lhy-20* single mutants were similar to that of *rve7-11* seedlings, and the *rve7-11 cca1-1* and *rve7-11 lhy-20* double mutants were indistinguishable from their constituent single mutants (Figure 7A-D). However, the hypocotyls of the *rve7-11 cca1-1 lhy-20* triple mutant were shorter than those of the *rve7-11* single mutant and the *cca1-1 lhy-20* double mutant (Figure 7E-F). These results are consistent with the notion that RVE7 plays redundant roles with CCA1/LHY in controlling hypocotyl elongation under warm temperature conditions.

Discussion

Circadian rhythms are generated in plants via the input of light and temperature signals and are sustained by interconnected feedback loops (Creux and Harmer, 2019). One output pathway of the circadian clock controls diurnal hypocotyl growth (Farre, 2012). Accumulating evidence indicates that the circadian clock is tightly associated with the adaptive growth of hypocotyls in plants (Gil and Park, 2019). CCA1 and LHY are core components of the circadian clock. The loss of CCA1 and LHY function confers early flowering at ambient temperatures (Mizoguchi et al., 2002) and reduces hypocotyl growth at warm temperatures (Figure 7). The genetic inactivation of *RVE1*, a paralog of *CCA1/LHY*, did not affect circadian rhythms, but did lead to a short-hypocotyl

phenotype at normal ambient growth temperature (Rawat et al., 2009). The constitutive overexpression of *RVE2* (also named *CIRCADIAN 1* [*CIR1*]) leads to a shorter circadian period, delayed flowering, and long hypocotyls at ambient temperature (Zhang et al., 2007). By contrast, the *rve4 rve6 rve8* triple mutant has a longer circadian period, delayed flowering, and a long hypocotyl phenotype at normal growth temperature (Gray et al., 2017), suggesting that RVE4/6/8 play a role opposite from that of CCA1/LHY/RVE1/RVE2 under ambient temperature conditions.

In the current study, we demonstrated that RVE7 is functionally redundant with CCA1/LHY under warm temperatures and is involved in thermoresponsive hypocotyl growth (Figure 8). These findings expand our understanding of the functions of the RVE protein family and highlight the connection between circadian clock control with thermomorphogenesis.

Previous studies have indicated that RVE1, RVE2, and RVE7 are not closely associated with the circadian oscillator, but these experiments have been carried out under normal growth conditions (Kuno et al., 2003; Rawat et al., 2009). In the current study, RVE7 showed transcriptional repression activity and directly inhibited the expression of circadian clock genes, including *ELF4*, at warm temperatures (Figure 4 and Figure 5). ELF4 is one of three components of the EC (Huang and Nusinow, 2016). ELF4 accelerates the nuclear localization of ELF3, which functions as a scaffolding protein to bring ELF4 together with LUX, a MYB domain transcription factor that directly binds to DNA (Nusinow et al., 2011; Herrero et al., 2012; Silva et al., 2020). The EC inhibits the expression of *PIF4* and *PIF5*, which is suppressed at dawn; therefore, elevated levels of PIF4 and/or PIF5 promote gene expression associated with hypocotyl growth (Nomoto et al., 2012). ELF3 also inhibits the activity of PIF4 independently of the EC (Nieto et al., 2015), which is released

by warm temperatures (Jung et al., 2020; Zhang et al., 2021b; Zhang et al., 2021c).

The expression of *ELF4* was not highly responsive to 29°C treatment in WT seedlings, but it was altered in both *RVE7* overexpression lines and *RVE7* mutant seedlings (Figure 4), suggesting that other unknown regulators function in an opposite manner to RVE7 to maintain *ELF4* expression at warm temperatures in the WT. When this balance is disrupted due to reduced or enhanced levels of *RVE7* transcript levels under warm conditions, the expression levels of *ELF4* and other downstream genes are likewise altered, leading to the phenotypes observed in the current study.

Interestingly, *LUX* transcript accumulation was fully responsive to 29°C conditions in various *RVE7* genotypes as in WT seedlings. This observation supports the notion that RVE7 and other factors that regulate the response to warm temperatures are required to counteract the upregulation of *LUX* under warm conditions. The EC has previously been shown to be crucial for this type of autoregulation, whereby ELF3 is subjected to protein degradation, leading to reduced EC activity under warm conditions (Ding et al., 2018; Zhang et al., 2021b; Zhang et al., 2021c). The current findings support the notion that RVE7 is essential for regulating *ELF4* expression under warm temperature conditions. Thus, in addition to ELF3 levels, the regulation of ELF4 levels is also essential for thermomorphogenic growth in plants.

We showed that *RVE7* transcript levels increase as RVE7 protein levels increased at 29°C (Figure 1A-B), supporting the role of RVE7 in plant responses to warm temperature conditions. The expression levels of *ELF4* were reduced in *RVE7ox-1* seedlings, which is consistent with the increased PIF4 accumulation and the increased expression of *PIF4* downstream genes in this line (Figure 2 and Figure 3). In addition, overexpressing *ELF4* substantially suppressed the hypocotyl phenotype of *RVE7ox-1* seedlings (Figure 6).

Therefore, the regulation of *ELF4* expression by RVE7 is important for thermoresponsive hypocotyl growth.

RVE7 regulates *ELF4* expression at dusk (ZT16) under warm conditions, as *ELF4* was expressed at higher levels at this time point in *rve7-11* seedlings than in the WT at 29°C (Figure 4B). The EC has previously been shown to inhibit PIF4 activity at both the transcriptional and posttranslational levels (Nomoto et al., 2012; Zhang et al., 2021a). Indeed, the protein abundance of PIF4 also decreased at dusk in *rve7-11* seedlings at 29°C relative to the WT (Figure 2E-F). We cannot exclude the possibility that RVE7 inhibits *PIF4* expression through other mechanisms under warm temperatures, as the expression of *PIF4* and its downstream genes was also reduced in *rve7-11* seedlings at 29°C at ZT24, when *ELF4* expression in this mutant showed little change from the WT (Figure 3 and Figure 4). Since RVE7 directly binds to the EE *cis*-elements in its target promoters (Figure 5C), and the EE is present in the promoters of many circadian clock genes (Nagel et al., 2015), besides *ELF4*, RVE7 might also regulate *PIF4* expression via other clock components.

Conclusion

In summary, we propose a model describing the positive role of RVE7 in thermomorphogenesis (Figure 8). According to this model, RVE7 represses the expression of *ELF4*, encoding an important component of the EC, to negatively regulate PIF4 levels during thermoresponsive hypocotyl growth.

Materials and Methods

Plant materials and hypocotyl length measurements

All Arabidopsis (*Arabidopsis thaliana*) genotypes used in this study were in the Columbia-0 (Col-0) background. The *cca1-1*, *elf4-209*, *hsfa1qk*, *lhy-20*, and *pif4-101* lines were described previously (Kolmos et al., 2009; Zhang et al.,

2013; Ding et al., 2018; Han et al., 2020). The *rve7* single mutants were generated using the CRISPR/Cas9 system (Yan et al., 2015). Two mutant alleles were selected for analysis: *rve7-11*, with a 16-bp deletion in the coding sequence; and *rve7-12*, with a 1-bp insertion in the coding sequence (Figure S4). Both mutations lead to a frame shift and premature termination of translation (Figure S4). To produce the overexpression lines, the coding sequences of *RVE7* and *ELF4* were amplified and inserted into pSKM36 or pCAMBIA1306, respectively. These constructs were subsequently transformed into Agrobacterium (*Agrobacterium tumefaciens*) strain GV3101 via the freeze-thaw method and introduced into plants via the floral-dip method (Clough and Bent, 1998). Higher-order mutants were generated by genetic crossing, as mentioned in the text.

Seeds were surface sterilized for 15 min in 0.01% (w/v) sodium hypochlorite and washed four times with sterile water. The seeds were sown on half-strength Murashige and Skoog (MS) medium with vitamins (containing 1.2% [w/v] sucrose and 0.8% [w/v] agar, pH 5.7) and stratified at 4°C for 2 days, after which they were transferred to a standard plant incubator at 22°C under a 16-h-light/8-h-dark photoperiod (long-day conditions) and 60% relative humidity. For phenotypic assays, seedlings were grown at 22°C for 3 days and transferred to 29°C or maintained at 22°C for 4 days. To measure hypocotyl length, the seedlings were photographed, and the hypocotyl lengths of the seedlings were measured using ImageJ software (Zhang et al., 2021b; Zhang et al., 2021c). All primers used in this study are listed in Table S1.

RNA extraction and RT-qPCR

Five- or six-day-old seedlings grown at 22°C were transferred to 29°C at ZT0, while the control seedlings were maintained at 22°C. The seedlings were harvested at the indicated times and immediately frozen in liquid nitrogen for gene expression analysis. For comparisons between *RVE7ox-1* seedlings and

WT seedlings or between *rve7-11* seedlings and WT seedlings, the same batch of WT seedlings was used for the control. Total RNA was extracted from the samples using an RNA Prep Pure Plant kit (Tiangen, Beijing. China). For reverse transcription, 2 μg of RNA and oligo (dT) primers were used to synthesize first-strand cDNA in a 20-μL reaction using M-MLV reverse transcriptase (TaKaRa, Dalian, China). The resulting cDNAs were used for PCR or qPCR analysis. qPCR was performed using SuperReal PreMix Color (Tiangen, Beijing, China) with a CFX96 real-time system (Bio-Rad, CA, USA) with the gene-specific primers listed in Table S1.

ChIP-qPCR

The ChIP assay was performed using an integrated method with a Chelex resin-based ChIP procedure and protein A agarose beads (Millipore, CA, USA) using an anti-myc antibody (Abmart, Shanghai, China). *RVE7-MYC* overexpression lines were grown for 13 days and transferred to 29°C or maintained at 22°C for the indicated times. The samples were fixed in 1% (w/v) formaldehyde for 2×10 min under a vacuum, and fixation was stopped by adding 0.15 M glycine to a final concentration of 0.125 M. The materials were then frozen in liquid nitrogen. After sonication in 0.8% (w/v) SDS buffer, protein A-agarose beads (Millipore, CA, USA) and an anti-MYC antibody were used to precipitate the DNA; IgG served as a serum control. The purified DNA was quantified by qPCR. All primers used for qPCR are listed in Table S1.

Immunoblot analysis

To analyze protein abundance, total proteins were extracted from the samples in extraction buffer (125 mM Tris-HCl [pH 8.0], 375 mM NaCl, 2.5 mM EDTA, 1% [w/v] SDS and 1% [w/v] beta-mercaptoethanol), and the protein concentrations were determined using a bicinchoninic acid assay (BCA) protein assay kit (Solarbio, Shanghai, China). The proteins were separated by 10% (w/v) SDS-PAGE and analyzed by immunoblotting using anti-MYC, anti-FLAG

(Abmart, Shanghai, China), anti-tubulin (Sigma, CA, USA), or anti-PIF4 (Abiocode, Shanghai, China) antibodies. The blots were scanned, and the densitometry signal intensity of each band was quantified using ImageJ software. The results are from the analyses of three immunoblots.

Electrophoretic Mobility Shift Assay (EMSA)

The coding sequence of *RVE7* was subcloned into pETMAL-H to produce and purify the recombinant MBP-RVE7 fusion protein according to standard protocols (Zhang et al., 2021c). The DNA (–264 to –301 bp relative to the TSS) containing the EE (5′-AAATATCT-3′) derived from the *ELF4* promoter was synthesized and biotinylated using a biotin 3′-end DNA Labeling Kit (Thermo Fisher Scientific, CA, USA). A mutated form of the EE (5′-AAATCGAG-3′) was used for the competition experiment. EMSA was performed using a LightShift Chemiluminescent EMSA Kit (Thermo Fisher Scientific, CA, USA) according to the manufacturer's protocols. Briefly, each binding reaction (20 mM HEPES, pH 7.2, 80 mM KCl, 0.1 mM EDTA, 10% [v/v] glycerol, 2.5 mM DTT, 0.07 mg/mL BSA, 8 ng/mL poly dI-dC) was incubated for 20 min at room temperature, and the reaction mixtures were resolved by electrophoresis through a 5% (w/v) non-denaturing polyacrylamide gel. After transferring to a nylon membrane, the membrane was crosslinked under UV light and examined with a Chemiluminescent Nucleic Acid Detection Module (Thermo Fisher Scientific, CA, USA).

Effector-reporter assay

The *ELF4* promoter sequence (–1,150 to +3 bp relative to the TSS) was PCR amplified and cloned into pGreen0800-II upstream of the firefly luciferase gene but downstream of the CaMV promoter to generate the reporter vector; the Renilla luciferase gene driven by the 35S promoter served as an internal control. The coding sequence of *RVE7* or *CCA1* was inserted into the pSKM36 vector to generate the respective effector construct. Different combinations of

constructs were transiently infiltrated in *Nicotiana benthamiana* leaves via Agrobacterium (strain GV3101)-mediated infiltration. Three days after infiltration, luciferase activity was measured with a Dual-luciferase Reporter Assay kit (Promega, CA, USA). All primers are listed in Table S1.

Acknowledgements

This project was financially supported by grants from Zhejiang Provincial Talent Program (2019R52005), the Fundamental Research Funds for the Zhejiang Provincial Universities (2021XZZX023), the 111 Project (B14027), and the BBSRC (BB/N018540/1). We would like to thank Drs. Xiaodong Xu (Henan University) and Wenqiang Tang (Hebei Normal University) for sharing the *cca1-1 lhy-20* and *hsfa1qk* mutant seeds, respectively.

Author contributions

J.X.L. and Y.Y.T. designed the experiments; Y.Y.T., W.L., M. J. W, and J.Y. L. performed the experiments; J.X.L. and Y.Y.T. analyzed the data; J.X.L. and S.J.D wrote the paper.

Declaration of interests

The authors declare no competing interests.

Data availability statement

The data that support the findings of this study are available in the supplementary materials of this article.

References

Box, M.S., Huang, B.E., Domijan, M., Jaeger, K.E., Khattak, A.K., Yoo, S.J., Sedivy, E.L., Jones, D.M., Hearn, T.J., Webb, A.A.R., Grant, A., Locke, J.C.W., and Wigge, P.A. (2015). ELF3 controls thermoresponsive growth in *Arabidopsis*. *Curr. Biol.* **25**: 194-199.

Casal, J.J., and Balasubramanian, S. (2019). Thermomorphogenesis. *Annu. Rev. Plant Biol.* **70**: 321-346.

Chung, B.Y.W., Balcerowicz, M., Di Antonio, M., Jaeger, K.E., Geng, F., Franaszek, K., Marriott, P., Brierley, I., Firth, A.E., and Wigge, P.A. (2020). An RNA thermoswitch regulates daytime growth in *Arabidopsis*. *Nat. Plants* **6**: 522-532.

Clough, S.J., and Bent, A.F. (1998). Floral dip: A simplified method for Agrobacterium-mediated transformation of *Arabidopsis thaliana*. *Plant J.* **16**: 735-743.

Creux, N., and Harmer, S. (2019). Circadian rhythms in plants. *Cold Spring Harb. Perspect. Biol.* **11**: a034611.

Ding, L., Wang, S., Song, Z.T., Jiang, Y., Han, J.J., Lu, S.J., Li, L., and Liu, J.X. (2018). Two B-box domain proteins, BBX18 and BBX23, interact with ELF3 and regulate thermomorphogenesis in *Arabidopsis*. *Cell Rep.* **25**: 1718-1728.

Farre, E.M. (2012). The regulation of plant growth by the circadian clock. *Plant Biol.* **14**: 401-410.

Fiorucci, A.S., Galvao, V.C., Ince, Y.C., Boccaccini, A., Goyal, A., Allenbach Petrolati, L., Trevisan, M., and Fankhauser, C. (2020). PHYTOCHROME INTERACTING FACTOR 7 is important for early responses to elevated temperature in *Arabidopsis* seedlings. *New Phytol.* **226**: 50-58.

Franklin, K.A., Lee, S.H., Patel, D., Kumar, S.V., Spartz, A.K., Gu, C., Ye, S., Yu, P., Breen, G., Cohen, J.D., Wigge, P.A., and Gray, W.M. (2011). PHYTOCHROME-INTERACTING FACTOR 4 (PIF4) regulates auxin biosynthesis at high temperature. *Proc. Natl. Acad. Sci. U.S.A.* **108**: 20231-20235.

Gil, K.E., and Park, C.M. (2019). Thermal adaptation and plasticity of the plant circadian clock. *New Phytol.* **221**: 1215-1229.

Gray, J.A., Shalit-Kaneh, A., Chu, D.N., Hsu, P.Y., and Harmer, S.L. (2017). The REVEILLE clock genes inhibit growth of juvenile and adult plants by control of cell size. *Plant Physiol.* **173**: 2308-2322.

Gray, W.M., Ostin, A., Sandberg, G., Romano, C.P., and Estelle, M. (1998). High temperature promotes auxin-mediated hypocotyl elongation in *Arabidopsis*. *Proc. Natl. Acad. Sci. U.S.A.* **95**: 7197-7202.

Han, S.H., Park, Y.J., and Park, C.M. (2020). HOS1 activates DNA repair systems to enhance plant thermotolerance. *Nat. Plants* **6**: 1439-1446.

Herrero, E., Kolmos, E., Bujdoso, N., Yuan, Y., Wang, M., Berns, M.C., Uhlworm, H., Coupland, G., Saini, R., Jaskolski, M., Webb, A., Goncalves, J., and Davis, S.J. (2012). EARLY FLOWERING4 recruitment of EARLY FLOWERING3 in the nucleus sustains the Arabidopsis circadian clock. *Plant Cell* **24**: 428-443.

Huang, H., and Nusinow, D.A. (2016). Into the Evening: Complex interactions in the Arabidopsis circadian clock. *Trends Genet.* **32**: 674-686.

Jung, J.H., Barbosa, A.D., Hutin, S., Kumita, J.R., Gao, M., Derwort, D., Silva, C.S., Lai, X., Pierre, E., Geng, F., Kim, S.B., Baek, S., Zubieta, C., Jaeger, K.E., and Wigge, P.A. (2020). A prion-like domain in ELF3 functions as a thermosensor in *Arabidopsis*. *Nature* **585**: 256-260.

Jung, J.H., Domijan, M., Klose, C., Biswas, S., Ezer, D., Gao, M., Khattak, A.K., Box, M.S., Charoensawan, V., Cortijo, S., Kumar, M., Grant, A., Locke, J.C.W., Schaefer, E., Jaeger, K.E., and Wigge, P.A. (2016). Phytochromes function as thermosensors in *Arabidopsis*. *Science* **354**: 886-889.

Kikis, E.A., Khanna, R., and Quail, P.H. (2005). ELF4 is a phytochrome-regulated component of a negative-feedback loop involving the central oscillator components CCA1 and LHY. *Plant J.* **44**: 300-313.

Klose, C., Nagy, F., and Schaefer, E. (2020). Thermal reversion of plant phytochromes. *Mol. Plant* **13**: 386-397.

Koini, M.A., Alvey, L., Allen, T., Tilley, C.A., Harberd, N.P., Whitelam, G.C., and Franklin, K.A. (2009). High temperature-medated adaptations in plant architecture require the bHLH transcription factor PIF4. *Curr. Biol.* **19**: 408-413.

Kolmos, E., Nowak, M., Werner, M., Fischer, K., Schwarz, G., Mathews, S., Schoof, H., Nagy, F., Bujnicki, J.M., and Davis, S.J. (2009). Integrating ELF4 into the circadian system through combined structural and functional studies. *HFSP J.* **3**: 350-366.

Kuno, N., Moller, S.G., Shinomura, T., Xu, X.M., Chua, N.H., and Furuya, M. (2003). The novel MYB protein EARLY-PHYTOCHROME-RESPONSIVE1 is a component of a slave circadian oscillator in *Arabidopsis*. *Plant Cell* **15**: 2476-2488.

Legris, M., Klose, C., Burgie, E.S., Rojas, C.C., Neme, M., Hiltbrunner, A., Wigge, P.A., Schafer, E., Vierstra, R.D., and Casal, J.J. (2016). Phytochrome B integrates light and temperature signals in *Arabidopsis*. *Science* **354**: 897-900.

Lin, J.Y., Xu, Y., and Zhu, Z.Q. (2020). Emerging plant thermosensors: From RNA to protein. *Trends Plant Sci.* **25**: 1187-1189.

Lu, S.X., Webb, C.J., Knowles, S.M., Kim, S.H.J., Wang, Z.Y., and Tobin, E.M. (2012). CCA1 and ELF3 interact in the control of hypocotyl length and flowering time in *Arabidopsis*. *Plant Physiol.* **158**: 1079-1088.

Marshall, C.M., Tartaglio, V., Duarte, M., and Harmon, F.G. (2016). The Arabidopsis sickle mutant exhibits altered circadian clock responses to cool temperatures and temperature-dependent alternative splicing. *Plant Cell* **28**: 2560-2575.

Mizoguchi, T., Wheatley, K., Hanzawa, Y., Wright, L., Mizoguchi, M., Song, H.R., Carre, I.A., and Coupland, G. (2002). LHY and CCA1 are partially redundant genes required to maintain circadian rhythms in *Arabidopsis*. *Dev. Cell* **2**: 629-641.

Nagel, D.H., Doherty, C.J., Pruneda-Paz, J.L., Schmitz, R.J., Ecker, J.R., and Kay, S.A. (2015). Genome-wide identification of CCA1 targets uncovers an expanded clock network in *Arabidopsis*. *Proc. Natl. Acad. Sci. U.S.A.* **112**: E4802-E4810.

Nieto, C., Lopez-Salmeron, V., Daviere, J.M., and Prat, S. (2015). ELF3-PIF4 interaction regulates plant growth independently of the Evening Complex. *Curr. Biol.* **25**: 187-193.

Nomoto, Y., Kubozono, S., Yamashino, T., Nakamichi, N., and Mizuno, T. (2012). Circadian clock- and PIF4-controlled plant growth: A coincidence mechanism directly integrates a hormone signaling network into the photoperiodic control of plant architectures in *Arabidopsis thaliana*. *Plant Cell Physiol.* **53**: 1950-1964.

Nusinow, D.A., Helfer, A., Hamilton, E.E., King, J.J., Imaizumi, T., Schultz, T.F., Farre, E.M., and Kay, S.A. (2011). The ELF4-ELF3-LUX complex links the circadian clock to diurnal control of hypocotyl growth. *Nature* **475**: 398-402.

Quint, M., Delker, C., Franklin, K.A., Wigge, P.A., Halliday, K.J., and van Zanten, M. (2016). Molecular and genetic control of plant thermomorphogenesis. *Nat. Plants* **2**: 15190.

Rawat, R., Takahashi, N., Hsu, P.Y., Jones, M.A., Schwartz, J., Salemi, M.R., Phinney, B.S., and Harmer, S.L. (2011). REVEILLE8 and PSEUDO-REPONSE REGULATOR5 form a negative feedback loop within the Arabidopsis circadian clock. *PLoS Genet.* **7**: e1001350.

Rawat, R., Schwartz, J., Jones, M.A., Sairanen, I., Cheng, Y., Andersson, C.R., Zhao, Y., Ljung, K., and Harmer, S.L. (2009). REVEILLE1, a Myb-like transcription factor, integrates the circadian clock and auxin pathways. *Proc. Natl. Acad. Sci. U.S.A.* **106**: 16883-16888.

Salome, P.A., Weigel, D., and McClung, C.R. (2010). The role of the Arabidopsis morning loop components CCA1, LHY, PRR7, and PRR9 in temperature compensation. *Plant Cell* **22**: 3650-3661.

Shalit-Kaneh, A., Kumimoto, R.W., Filkov, V., and Harmer, S.L. (2018). Multiple feedback loops of the Arabidopsis circadian clock provide rhythmic robustness across environmental conditions. *Proc. Natl. Acad. Sci. U.S.A.* **115**: 7147-7152.

Silva, C.S., Nayak, A., Lai, X., Hutin, S., Hugouvieux, V., Jung, J.H., Lopez-Vidriero, I., Franco-Zorrilla, J.M., Panigrahi, K.C.S., Nanao, M.H., Wigge, P.A., and Zubieta, C. (2020). Molecular mechanisms of Evening Complex activity in *Arabidopsis*. *Proc. Natl. Acad. Sci. U.S.A.* **117**: 6901-6909.

Sun, J., Tian, Y., Lian, Q., and Liu, J.X. (2020). Mutation of *DELAYED GREENING1* impairs chloroplast RNA editing at elevated ambient temperature in *Arabidopsis*. *J. Genet. Genom.* **47**: 201-212.

Sun, J., Qi, L., Li, Y., Chu, J., and Li, C. (2012). PIF4-mediated activation of *YUCCA8* expression integrates temperature into the auxin pathway in regulating Arabidopsis hypocotyl growth. *PLoS Genet.* **8**: 201-212.

Sun, Q.B., Wang, S.L., Xu, G., Kang, X.J., Zhang, M., and Ni, M. (2019). SHB1 and CCA1 interaction desensitizes light responses and enhances thermomorphogenesis. *Nat. Commun.* **10**: 3110.

Thines, B., and Harmon, F.G. (2010). Ambient temperature response establishes ELF3 as a required component of the core Arabidopsis circadian clock. *Proc. Natl. Acad. Sci. U.S.A.* **107**: 3257-3262.

Vu, L.D., Xu, X., Gevaert, K., and Smet, I. (2019). Developmental plasticity at high temperature. *Plant Physiol.* **181**: 399-411.

Wang, M.J., Ding, L., Liu, X.H., and Liu, J.X. (2021). Two B-box domain proteins, BBX28 and BBX29, regulate flowering time at low ambient temperature in *Arabidopsis*. *Plant Mol. Biol.* **106**: 21-32.

Wang, S., Ding, L., Liu, J.X., and Han, J.J. (2018). PIF4-regulated thermo-responsive genes in *Arabidopsis*. *Biotech. Bulletin* **34**: 57-65.

Xie, Q.G., Wang, P., Liu, X., Yuan, L., Wang, L.B., Zhang, C.G., Li, Y., Xing, H.Y., Zhi, L.Y., Yue, Z.L., Zhao, C.S., McClung, C.R., and Xu, X.D. (2014). LNK1 and LNK2 are transcriptional coactivators in the Arabidopsis circadian oscillator. *Plant Cell* **26**: 2843-2857.

Yamashino, T., Ito, S., Niwa, Y., Kunihiro, A., Nakamichi, N., and Mizuno, T. (2008). Involvement of Arabidopsis clock-associated pseudo-response regulators in diurnal oscillations of gene expression in the presence of environmental time cues. *Plant Cell Physiol*. **49**: 1839-1850.

Yan, L., Wei, S., Wu, Y., Hu, R., Li, H., Yang, W., and Xie, Q. (2015). High-efficiency genome editing in Arabidopsis using *YAO* promoter-driven CRISPR/Cas9 system. *Mol. Plant* **8**: 1820-1823.

Zhang, C., Xie, Q.G., Anderson, R.G., Ng, G.N., Seitz, N.C., Peterson, T., McClung, C.R., McDowell, J.M., Kong, D.D., Kwak, J.M., and Lu, H.

(2013). Crosstalk between the circadian clock and innate immunity in *Arabidopsis*. *PLoS Pathog*. **9**: e1003370.

Zhang, L.L., Luo, A., Davis, S.J., and Liu, J.X. (2021a). Timing to grow: Roles of clock in thermomorphogenesis. *Trends Plant Sci.* **26**: 1248-1257.

Zhang, L.L., Li, W., Tian, Y.Y., Davis, S.J., and Liu, J.X. (2021b). The E3 ligase XBAT35 mediates thermoresponsive hypocotyl growth by targeting ELF3 for degradation in *Arabidopsis*. *J. Integr. Plant Biol.* **63**: 1097-1103.

Zhang, L.L., Shao, Y.J., Ding, L., Wang, M.J., Davis, S.J., and Liu, J.X. (2021c). XBAT31 regulates thermoresponsive hypocotyl growth through mediating degradation of the thermosensor ELF3 in *Arabidopsis*. *Sci. Adv.* **7**: eabf4427.

Zhang, X., Chen, Y., Wang, Z.Y., Chen, Z., Gu, H., and Qu, L.J. (2007). Constitutive expression of CIR1 (RVE2) affects several circadian-regulated processes and seed germination in *Arabidopsis*. *Plant J.* **51**: 512-525.

Supplemental information

Additional Supporting Information may be found online in the Supporting Information section at the end of the article:

Figure S1. Warm temperature–regulated *CCA1*, *LHY*, and *RVE* gene expression. Six-day-old wild-type (WT) seedlings grown at 22°C were maintained at 22°C or transferred to 29°C and sampled at the indicated time points for gene expression analysis. Relative gene expression is the expression level of the target gene normalized to that of *PP2A*. Data are means ± standard error (SE, n = 3).

Figure S2. Validation of transgenic lines. Six-day-old wild-type (WT), *pif4-101*, and various transgenic overexpression lines grown at 22°C were maintained at 22°C or transferred to 29°C and sampled at ZT24 for RT-PCR analysis. The expression of *UBQ5* was used as an internal control.

Figure S3. Protein stability assay. Seven-day-old *RVE7ox-1* seedlings grown at 22°C were maintained at 22°C or transferred to 29°C for 16 h in the presence or absence of the 26S proteasome inhibitor MG132 and sampled for immunoblotting with anti-myc antibody. Tubulin served as a protein loading control.

Figure S4. Characterization of gene-edited *rve7* mutant plants. Alignment of the partial coding sequences of *RVE7* and their deduced amino acid sequences in the wild type (WT) and the *rve7* mutants (*rve7-11* and *rve7-12*). The sgRNA sequences used for vector construction are shown in red. *, stop codon.

Figure S5. Expression patterns of *RVE7*, *ELF4*, and *PIF4*. Five-day-old wild-type (WT) seedlings grown at 22°C were maintained at 22°C or transferred to 29°C and sampled at different time points (ZT) for gene expression analysis. The expression level of each gene was normalized to that of *PP2A*. Data are means ± SE (n = 3).

Figure S6. Binding of RVE7 to the *PIF4* promoter. Thirteen-day-old transgenic seedlings overexpressing *RVE7-MYC* grown at 22°C were maintained at 22°C or transferred to 29°C for 16 h and sampled for ChIP-qPCR using anti-MYC antibody. Relative enrichment of each sample was normalized to that the anti-GST sample (IgG control) at 16 h at 22°C, both of which were normalized to the *TA3* control. Data are means ± SE (n = 3). Different letters above the bars indicate significant differences, as determined by post hoc test ($P < 0.05$).

Table S1. Primers used in this study.

720 **FIGURE LEGENDS**

721 **Figure 1. *RVE7* is responsive to warm temperatures and positively**
722 **regulates thermomorphogenesis. A-B**, Upregulation of *RVE7* transcript
723 levels by warm temperatures. Six-day-old wild-type (WT) seedlings grown at
724 22°C were maintained at 22°C or transferred to 29°C at ZT0 and sampled at
725 the indicated time for gene expression analysis (A). The *hsfa1a hsfa1b hsfa1c*
726 *hsfa1d* quadruple mutant (*hsfa1qk*) was also treated like the WT and sampled
727 at ZT24 (B). Relative gene expression is the expression level of *RVE7* in each
728 sample normalized to that of *PP2A*. Data are means ± SE (n = 3). **C**,
729 Accumulation of RVE7 under warm temperature conditions. Seven-day-old
730 *RVE7-MYC* overexpression seedlings grown at 22°C were maintained at 22°C
731 or transferred to 29°C and sampled for immunoblotting with anti-myc antibody.
732 Tubulin served as a protein loading control. **D-G**, Phenotypic analysis.
733 Seedlings of WT, *RVE7* loss-of-function mutants (*rve7-11* and *rve7-12*), and
734 *RVE7* overexpression lines (*RVE7ox-1* and *RVE7ox-2*) were grown at 22°C for
735 3 days and kept at 22°C or transferred to 29°C for 4 days, after which
736 representative seedlings were imaged (D-E) and their hypocotyl lengths
737 measured (F-G). *pif4-101* was used as a control. Data are means ± standard
738 deviation (SD, n = 24). Different lowercase letters indicate significant
739 differences, as determined by post hoc test ($P < 0.05$). Scale bars = 5 mm.

740 **Figure 2. RVE7 functions upstream of PIF4 in thermomorphogenesis. A-**
741 **D**, Genetic analysis of the roles of *RVE7* and *PIF4* in thermoresponsive
742 hypocotyl growth. Seedlings of the WT, *rve7-11*, *pif4-101*, the *rve7-11 pif4-101*
743 double mutant, *RVE7ox*, and *pif4-101 RVE7ox* were grown at 22°C for 3 days
744 and kept at 22°C or transferred to 29°C for 4 days, after which representative
745 seedlings were imaged (A-B) and their hypocotyl lengths measured (C-D). Data
746 are means ± SD (n = 24). Scale bars = 5 mm. **E-F**, Accumulation of PIF4.
747 Seven-day-old WT, *rve7-11*, and *RVE7ox-1* seedlings grown at 22°C were

maintained at 22°C or transferred to 29°C for 16 h and sampled for immunoblotting with anti-PIF4 antibody (E). Tubulin served as a protein loading control. The band intensities in three immunoblots were quantified (F). Data are means ± SE (n = 3). Different lowercase letters indicate significant differences, as determined by post hoc test ($P < 0.05$).

Figure 3. RVE7 regulates the expression of *PIF4* and its downstream genes under warm conditions. A-J, Expression of *PIF4* and its downstream genes under ambient and warm temperature conditions. Five-day-old WT, *rve7-11*, and *RVE7ox-1* seedlings grown at 22°C were maintained at 22°C or transferred to 29°C and sampled at three different time points (ZT) for quantitative gene expression analysis. The expression level of each gene was normalized to that of the WT at ZT16 at 22°C, which was normalized to that of *PP2A*. Data are means ± SE (n = 3).

Figure 4. RVE7 regulates EC gene expression under warm conditions. A-F, Expression of three EC genes under ambient and warm temperature conditions. Five-day-old WT, *rve7-11*, and *RVE7ox-1* seedlings grown at 22°C were maintained at 22°C or transferred to 29°C and sampled at three different time points (ZT) for quantitative gene expression analysis. The expression level of each gene was normalized to that of the WT at ZT16 at 22°C, which was normalized to that of *PP2A*. Data are means ± SE (n = 3).

Figure 5. RVE7 directly inhibits the expression of *ELF4*. A-B, Transcriptional repression activity assay. RVE7-MYC, CCA1-MYC, or MYC (vector control) driven by the 35S promoter was used as the effector, and the firefly luciferase driven by the *ELF4* promoter (pELF4) linked to the 35S promoter was co-expressed as the reporter in effector-reporter assays. The activity of Renilla luciferase, whose encoding gene was constitutively expressed, was used as an internal control. Relative luciferase activity is firefly luciferase activity normalized to Renilla luciferase activity, which was then

normalized to the vector control. Data are means ± SE (n = 3). **C**, Direct binding of RVE7 to the EE. Recombinant MBP-RVE7 was incubated with biotin-labeled DNA containing the EE (5′-AAATATCT-3′) derived from the *ELF4* promoter, and electrophoretic mobility shift assays (EMSAs) were performed. Non-labeled native or mutated (5′-AAATCGAG-3′) cold probes were added to the reaction for competition assays. **D,** Binding of RVE7 to the *ELF4* promoter in seedlings under two temperature conditions. Thirteen-day-old transgenic seedlings overexpressing *RVE7-MYC* grown at 22°C were maintained at 22°C or transferred to 29°C for 16 h and sampled for ChIP-qPCR using anti-MYC antibody. The relative enrichment of *ELF4* DNA in each sample was normalized to that in the anti-GST sample (IgG control) at 22°C, both of which were normalized to that of the *TA3* control. Data are means ± SE (n = 3). Different lowercase letters indicate significant differences, as determined by post hoc test ($P < 0.05$).

Figure 6. Overexpressing *ELF4* suppresses the long hypocotyl phenotype caused by *RVE7* overexpression under warm temperature conditions. A-F, Genetic analysis of the roles of *RVE7* and *ELF4* in thermomorphogenesis. Seedlings of WT, *rve7-11*, *elf4-209*, *rve7-11 elf4-209*, *RVE7*ox-1 and *ELF4* overexpression (*ELF4*ox-1) , *RVE7* and *ELF4* double overexpression (*ELF4*ox-1 *RVE7*ox-1) lines, and *elf4-209 RVE7ox-3* grown at 22°C for 3 days were kept at 22°C or transferred to 29°C for 4 days, after which representative seedlings were imaged (A, C, E) and their hypocotyl lengths measured (B, D, F). Data are means ± SD (n = 24). **G-H**, Accumulation of PIF4. Seven-day-old WT, *ELF4ox-21*, *RVE7ox-1*, and *RVE7ox-1 ELF4ox-11* seedlings grown at 22°C were maintained at 22°C or transferred to 29°C for 16 h and sampled for immunoblotting with anti-PIF4 antibody (G). Tubulin served as a protein loading control. The band intensities in three immunoblots were quantified (H). Data are

means ± SE (n = 3). Different lowercase letters indicate significant differences, as determined by post hoc test ($P < 0.05$). Scale bars = 5 mm.

Figure 7. RVE7 functions redundantly with CCA1/LHY in thermomorphogenesis. A-F, Genetic analysis of the roles of *RVE7* and *CCA1*/*LHY* in thermomorphogenesis. WT, *rve7-11*, *cca1-1*, *lhy-20*, *rve7-11 cca1-1*, *rve7-11 lhy-20*, and *rve7-11 cca1-1 lhy-20* seedlings grown at 22°C for 3 days were kept at 22°C or transferred to 29°C for 4 days, after which representative seedlings were imaged (A, C, E) and their hypocotyl lengths measured (B, D, F). Data are means ± SD (n = 24). Different lowercase letters indicate significant differences, as determined by post hoc test ($P < 0.05$); scale bars = 5 mm.

Figure 8. A simplified working model for the role of RVE7 in thermoresponsive hypocotyl growth. The hypocotyl growth–promoting bHLH transcription factor PIF4 is negatively regulated by the evening complex (EC) consisting of ELF3, ELF4, and LUX. Under warm temperature conditions (29°C), the MYB transcription factor RVE7 accumulates and reduces the expression of *ELF4*, allowing PIF4 to reach a certain level in wild-type (WT) seedlings. In *RVE7* overexpression (*RVE7*ox-1) seedlings, higher RVE7 protein abundance leads to lower *ELF4* transcript levels and higher accumulation of PIF4, thereby triggering higher expression of PIF4 downstream genes and faster hypocotyl growth under warm temperature conditions. By contrast, in *RVE7* mutant (*rve7-11*) seedlings, higher *ELF4* expression levels lead to greater repression of PIF4, resulting in shorter hypocotyls. The positive regulators of *ELF4* and *PIF4* expression are not depicted in the model. Positive and negative regulatory activities are indicated by arrows and lines with bars, respectively. The thickness of the lines and the depth of color of the shapes reflect the degree of regulation.

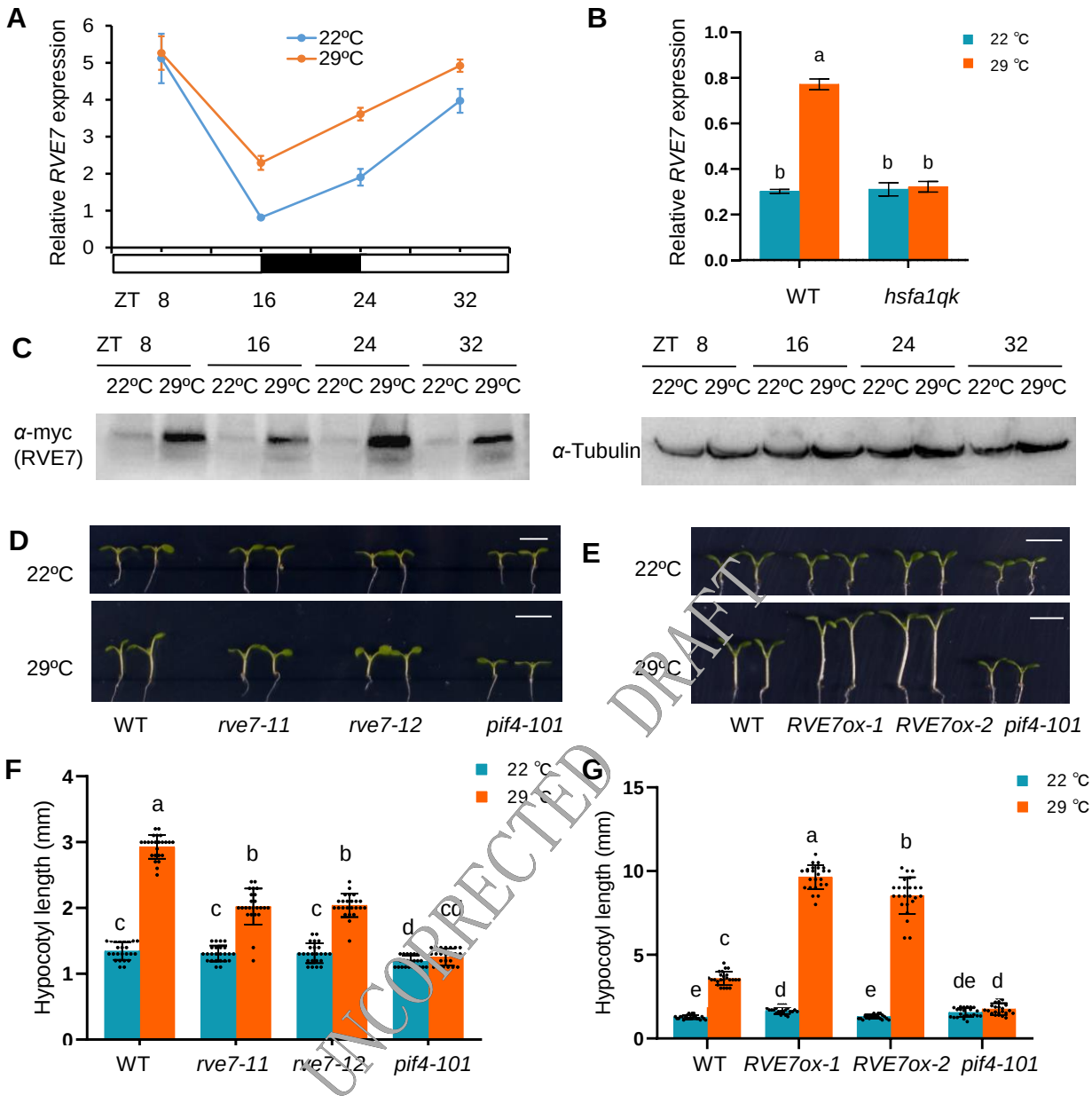

Figure 1. *RVE7* is responsive to warm temperatures and positively regulates thermomorphogenesis. A-B, Upregulation of *RVE7* transcript levels by warm temperatures. Six-day-old wild-type (WT) seedlings grown at 22° C were maintained at 22° C or transferred to 29° C at ZT0 and sampled at the indicated time for gene expression analysis (A). The *hsfa1a hsfa1b hsfa1c hsfa1d* quadruple mutant (*hsfa1qk*) was also treated like the WT and sampled at ZT 24 (B). Relative gene expression is the expression level of *RVE7* in each sample normalized to that of *PP2A*. Error Data are means ± SE (n=3). **C**, Accumulation of RVE7 under warm temperature conditions. Seven-day-old *RVE7-MYC* overexpression seedlings grown at 22° C were maintained at 22° C or transferred to 29° C and sampled for immunoblotting with anti-myc antibody. Tubulin served as a protein loading control. **D-G**, Phenotypic analysis. Seedlings of WT, *RVE7* loss-of-function mutants (*rve7-11* and *rve7-12*), and *RVE7* overexpression lines (*RVE7ox-1* and *RVE7ox-2*) were grown at 22° C for 3 days and kept at 22° C or transferred to 29° C for 4 days, after which representative seedlings were imaged (D-E) and their hypocotyl lengths measured (F-G). *pif4-101* was used as a control. Data are means ± standard deviation (SD, n=24). Different lowercase letters indicate significant differences, as determined by post hoc test ($P < 0.05$). Scale bars = 5 mm.

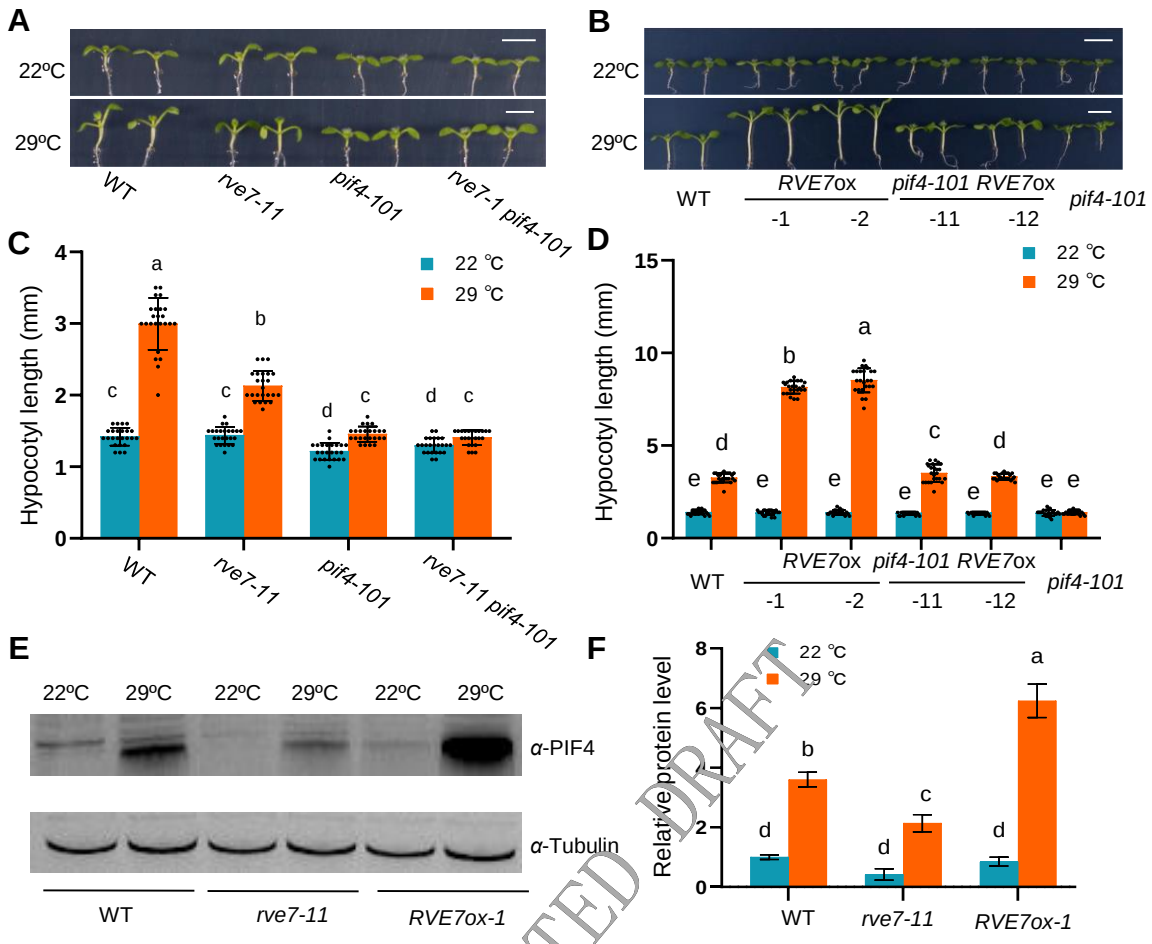

Figure 2. RVE7 functions upstream of PIF4 in thermomorphogenesis. A-D, Genetic analysis of the roles of *RVE7* and *PIF4* in thermoresponsive hypocotyl growth. Seedlings of the WT, *rve7-11*, *pif4-101*, the *rve7-11 pif4-101* double mutant, *RVE7ox* and *pif4-101 RVE7ox* were grown at 22° C for 3 days and kept at 22° C or transferred to 29° C for 4 days, after which representative seedlings were imaged (A-B) and their hypocotyl lengths measured (C-D). Data are means ± SD (n=24). Scale bars = 5 mm. **E-F**, Accumulation of PIF4. Seven-day-old WT, *rve7-11*, and *RVE7ox-1* seedlings grown at 22° C were maintained at 22° C or transferred to 29° C for 16 h and sampled for immunoblotting with anti-PIF4 antibody (E). Tubulin served as a protein loading control. The band intensities in three immunoblots were quantified (F). Data are means ± SE (n = 3). Different lowercase letters indicate significant differences, as determined by post hoc test ($P < 0.05$).

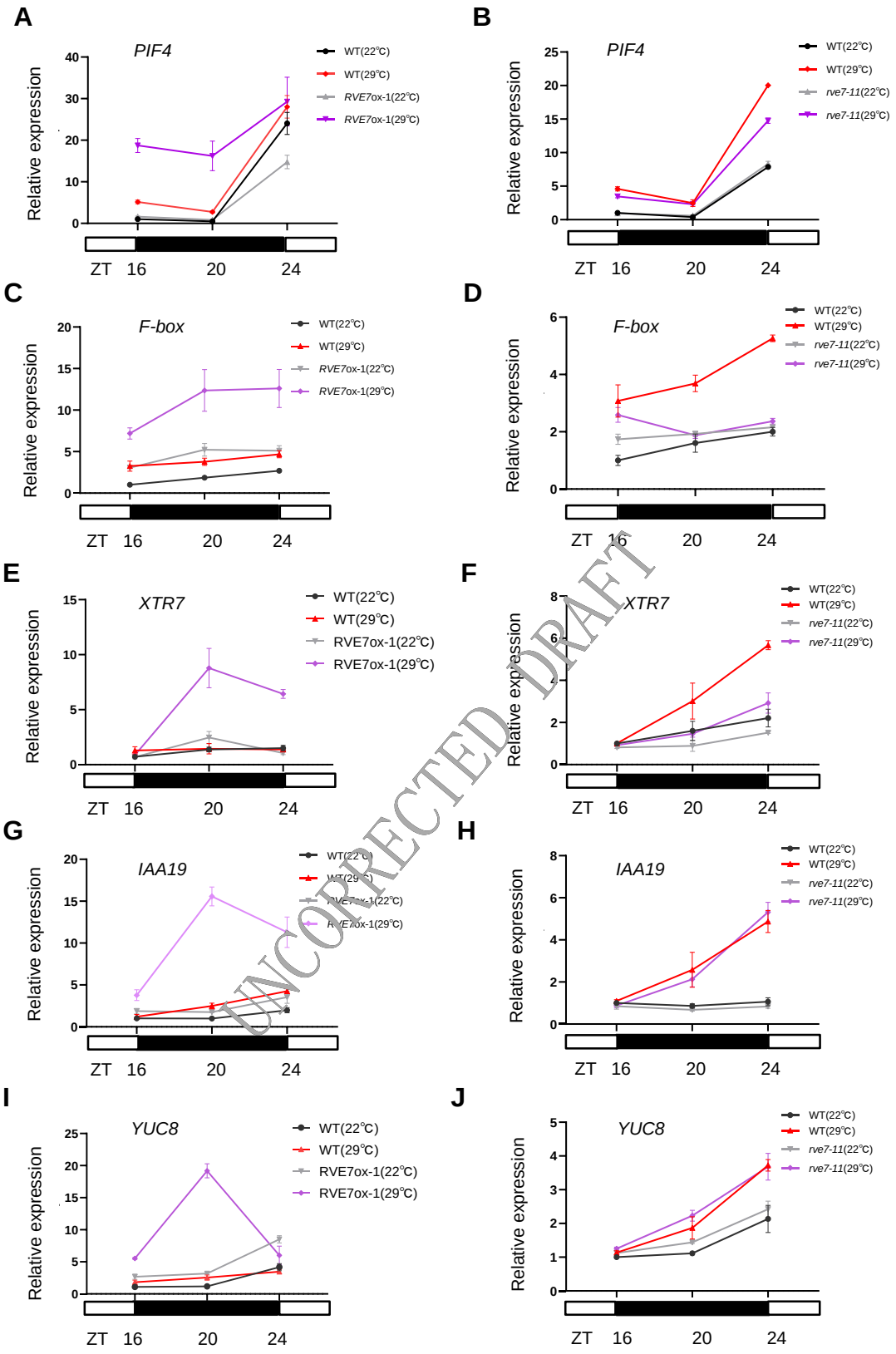

Figure 3. RVE7 regulates the expression of *PIF4* and its downstream genes under warm conditions. A-J, Expression of *PIF4* and its downstream genes under ambient and warm temperature conditions. Five-day-old WT, *rve7-11*, and *RVE7ox-1* seedlings grown at 22° C were maintained at 22° C or transferred to 29° C and sampled at three different time points (ZT) for quantitative gene expression analysis. The expression level of each gene was normalized to that of WT at ZT16 at 22° C, which was normalized to that of *PP2A*. Data are means ±SE (n = 3).

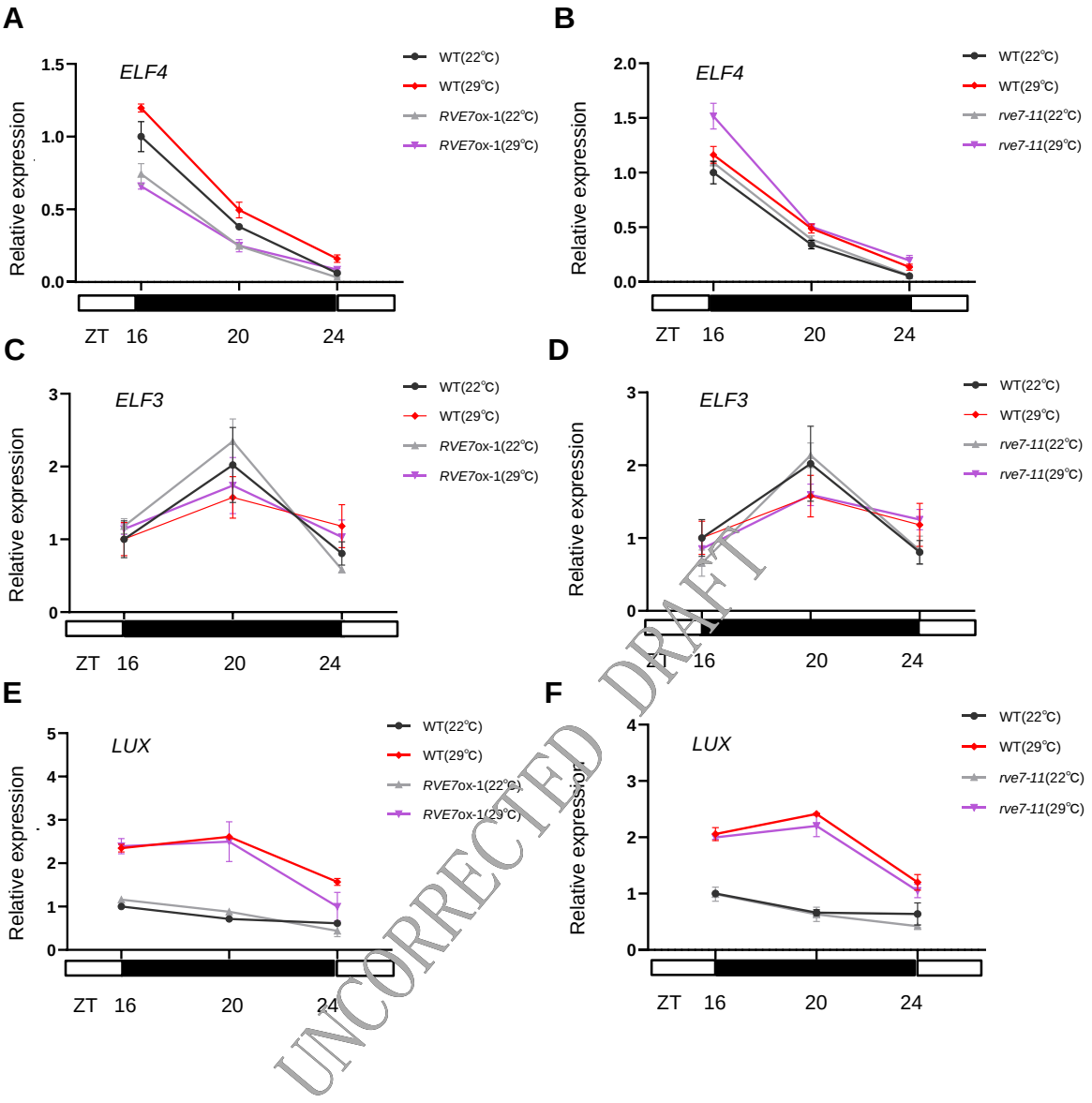

Figure 4. RVE7 regulates EC gene expression under warm conditions. A-F, Expression of three EC genes under ambient and warm temperature conditions. Five-day-old WT, *rve7-11* and *RVE7ox-1* seedlings grown at 22° C were maintained at 22° C or transferred to 29° C and sampled at three different time points (ZT) for quantitative gene expression analysis. The expression level of each gene was normalized to that of WT at ZT16 at 22° C, which was normalized to that of *PP2A*. Data are means ±SE (n = 3).

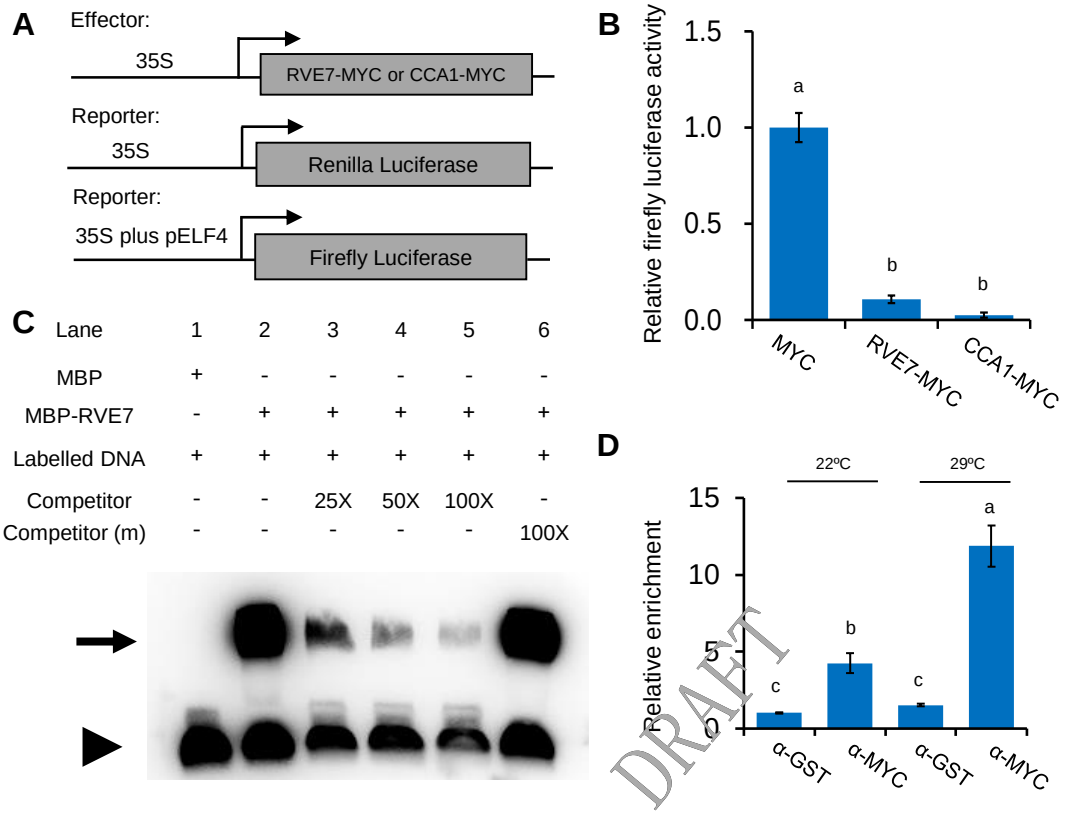

Figure 5. RVE7 directly inhibits the expression of *ELF4*. **A-B**, Transcriptional repression activity assay. RVE7-MYC, CCA1-MYC, or MYC (vector control) driven by the 35S promoter was used as the effector, and the firefly luciferase driven by the *ELF4* promoter (pELF4) linked to the 35S promoter was co-expressed as the reporter in effector-reporter assays. The activity of Renilla luciferase, whose encoding gene was constitutively expressed, was used as an internal control. Relative luciferase activity is firefly luciferase activity normalized to Renilla luciferase activity, which was then normalized to the vector control. Data are means ±SE (n = 3). **C**, Direct binding of RVE7 to the EE. Recombinant MBP-RVE7 was incubated with biotin-labeled DNA containing the EE (5'-AAATATCT-3') derived from the *ELF4* promoter and electrophoretic mobility shift assays (EMSAs) were performed. Non-labeled native or mutated (5'-AAATCGAG-3') cold probes were added to the reaction for competition assays. **D,** Binding of RVE7 to the *ELF4* promoter in seedlings under two temperature conditions. Thirteen-day-old transgenic seedlings overexpressing *RVE7-MYC* grown at 22° C were maintained at 22° C or transferred to 29° C for 16 h and sampled for ChIP-qPCR using anti-MYC antibody. The relative enrichment of *ELF4* DNA in each sample was normalized to that in the anti-GST sample (IgG control) at 22° C, both of which were normalized to that of the *TA3* control. Data are means ± SE (n = 3). Different lowercase letters indicate significant differences, as determined by post hoc test ($P < 0.05$).

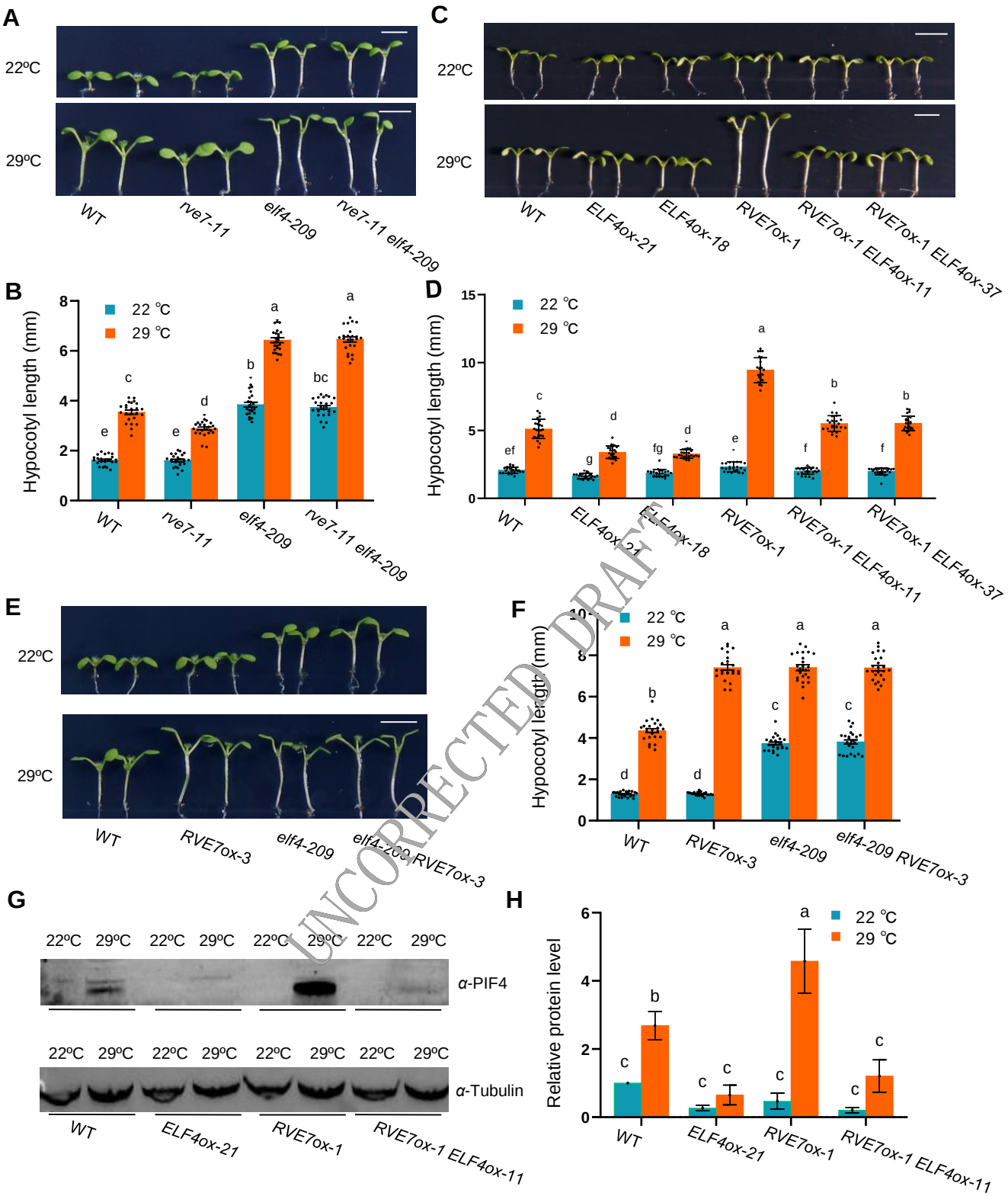

Figure 6. Overexpressing *ELF4* suppresses the long hypocotyl phenotype caused by *RVE7* overexpression under warm temperature conditions. A-F, Genetic analysis of the roles of *RVE7* and *ELF4* in thermomorphogenesis. Seedlings of WT, *rve7-11*, *elf4-209*, *rve7-11 elf4-209*, *RVE7*ox-1 and *ELF4* overexpression (*ELF4*ox-1) , *RVE7* and *ELF4* double overexpression (*ELF4*ox-1 *RVE7*ox-1) lines, and *elf4-209 RVE7ox-3* grown at 22° C for 3 days were kept at 22° C or transferred to 29° C for 4 days, after which representative seedlings were imaged (A, C, E) and their hypocotyl lengths measured (B, D, F). Data are means ± SD (n=24). **G-H**, Accumulation of PIF4. Seven-day-old WT, *ELF4ox-21*, *RVE7ox-1* and *RVE7ox-1 ELF4ox-11* seedlings grown at 22° C were maintained at 22° C or transferred to 29° C for 16 h and sampled for immunoblotting with anti-PIF4 antibody (G). Tubulin served as a protein loading control. The band intensities in three immunoblots were quantified (H). Data are means ± *SE* (n = 3). Different lowercase letters indicate significant differences, as determined by post hoc test ($P < 0.05$). Scale bars = 5 mm.

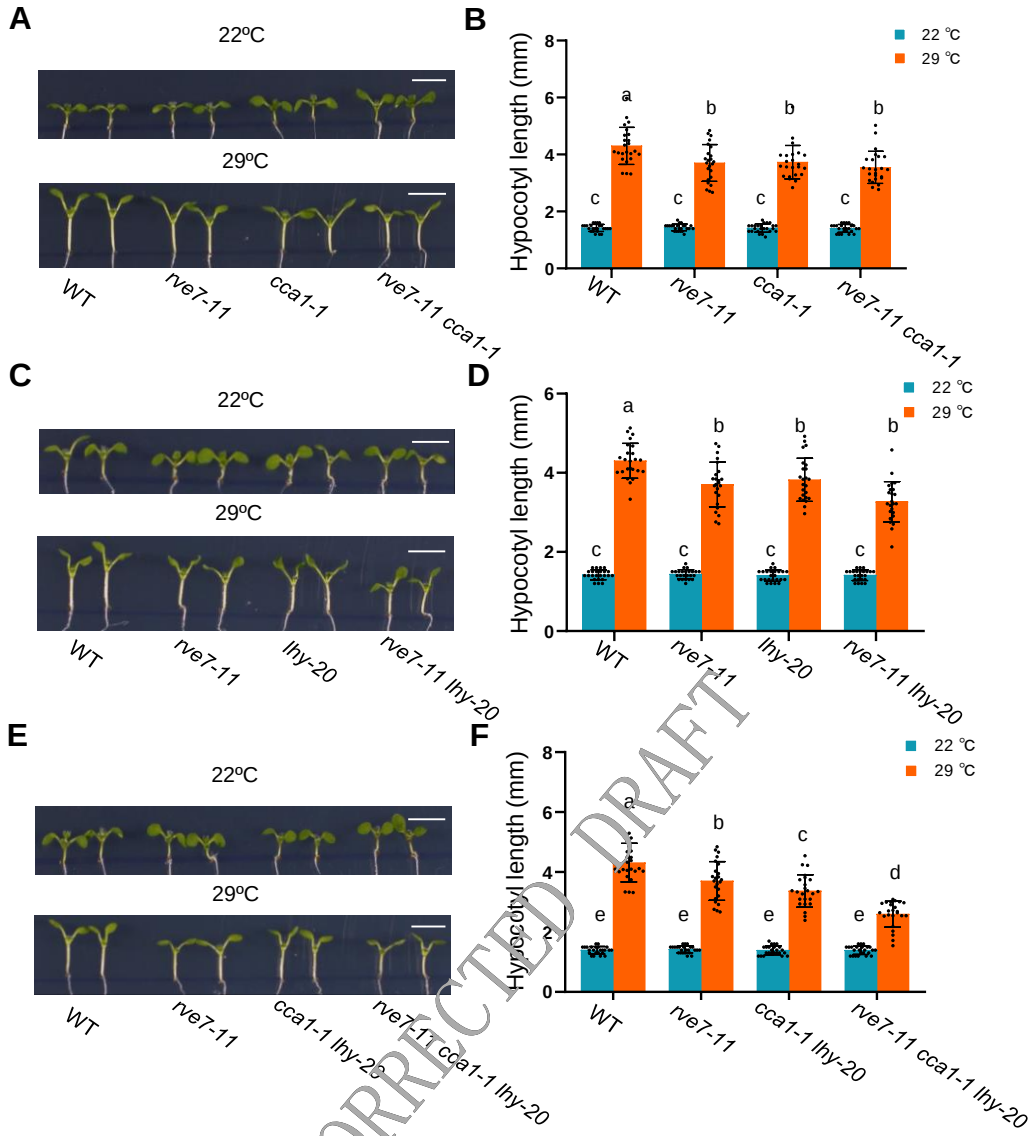

Figure 7. RVE7 functions redundantly with CCA1/LHY in thermomorphogenesis. A-F, Genetic analysis of the roles of *RVE7* and *CCA1/LHY* in thermomorphogenesis. WT, *rve7-11*, *cca1-1*, *lhy-20*, *rve7-11 cca1-1*, *rve7-11 lhy-20*, and *rve7-11 cca1-1 lhy-20* seedlings grown at 22° C for three days were kept at 22° C or transferred to 29° C for 4 days, after which representative seedlings were imaged (A, C, E), and their hypocotyl lengths measured (B, D, F). Data are means ± *SD* (n=24). Different lowercase letters indicate significant differences, as determined by post hoc test ($P < 0.05$); Scale bars = 5 mm.

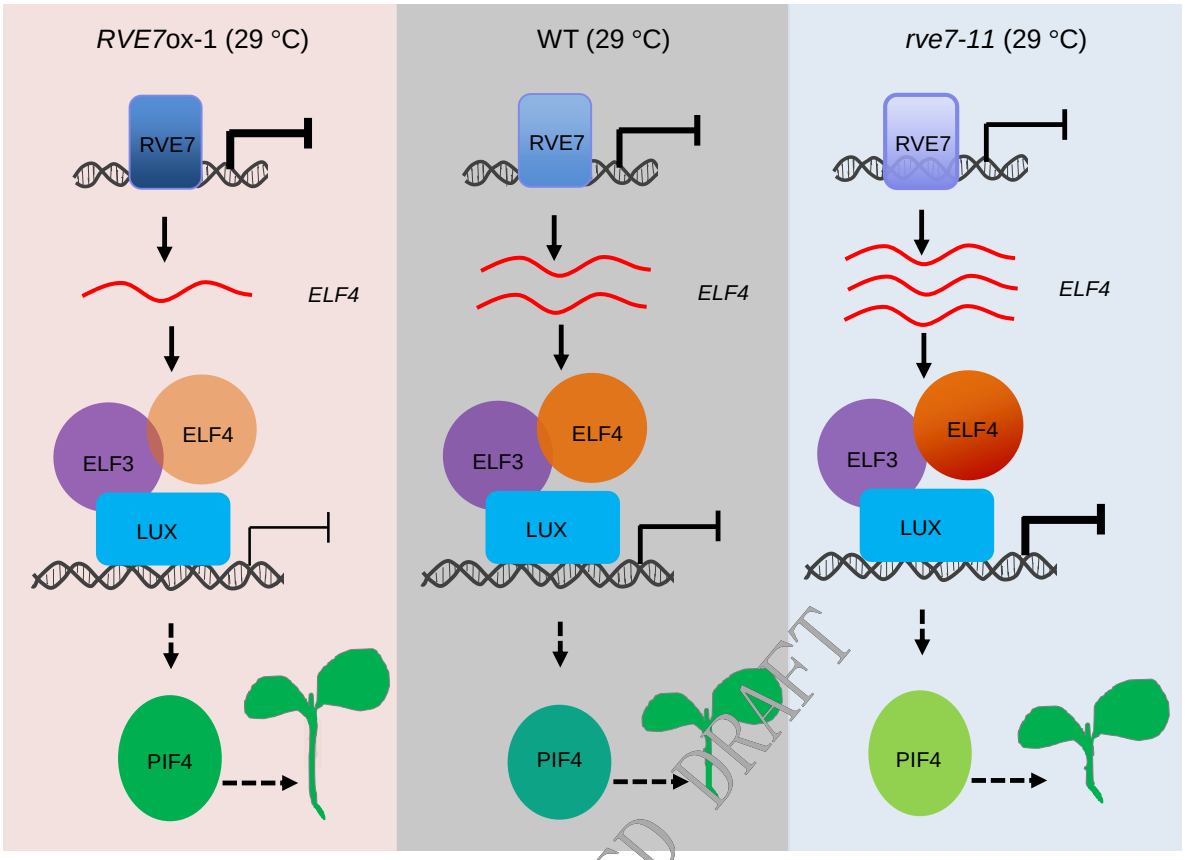

Figure 8. A simplified working model for the role of RVE7 in thermoresponsive hypocotyl growth. The hypocotyl growth-promoting bHLH transcription factor PIF4 is negatively regulated by the evening complex (EC) consisting of ELF3, ELF4, and LUX. Under warm temperature conditions (29° C), the MYB transcription factor RVE7 accumulates and reduces the expression of *ELF4*, allowing PIF4 to reach a certain level in wild-type (WT) seedlings. In *RVE7* overexpression (*RVE7*ox-1) seedlings, higher RVE7 protein abundance leads to lower *ELF4* transcript levels and higher accumulation of PIF4, thereby triggering higher expression of PIF4 downstream genes and faster hypocotyl growth under warm temperature conditions. By contrast, in *RVE7* mutant (*rve7-11*) seedlings, higher *ELF4* expression levels lead to greater repression of PIF4, resulting in shorter hypocotyls. The positive regulators of *ELF4* and *PIF4* expression are not depicted in the model. Positive and negative regulatory activities are indicated by arrows and lines with bars, respectively. The thickness of the lines and the depth of color of the shapes reflect the degree of regulation.